In-plane magnetization anisotropy in Gd_2CuO_4 single crystals

A. Butera and M. Tovar
Centro Atómico Bariloche and Instituto Balseiro, Comisión Nacional de Energía Atómica, 8400 S. C. de Bariloche, Argentina

S. B. Oseroff
San Diego State University, San Diego, California 92182

Z. Fisk
Los Alamos National Laboratory, Los Alamos, New Mexico 87545
(Received 6 June 1995)

We present here detailed dc magnetization measurements of a Gd_2CuO_4 single crystal. Besides the strong out-of-plane anisotropy that favors the orientation of the magnetization within the CuO_2 planes for R_2CuO_4, we have also found in-plane anisotropy when the external field H is applied parallel to the CuO_2 planes. Three regions could be distinguished in magnetization M vs field curves: for $0<H<H_c'\approx 35$ G, M is only slightly anisotropic. A metamagneticlike transition is observed when H is parallel to an anisotropy easy axis, coincident with one [110] direction. Above this transition a "hidden" weak ferromagnetic component develops. For $H_c'<H<H_c^*\approx 300$ G strong anisotropy is found, and above the critical field H_c^* all magnetic moments are completely aligned with the external field and the magnetization is again isotropic. Hysteretic behavior has been observed at the metamagnetic transition, probably due to the existence of weak ferromagnetic domains. An intraplanar anisotropy field $H_x\approx 1200$ G and an interplanar coupling constant $J_\perp\approx 2$ mK, have been estimated from the experimental critical fields using a mean field description of the magnetic coupling between CuO_2 planes.

I. INTRODUCTION

The compounds R_2CuO_4 (R = Pr,..., Yb) crystallize in the tetragonal T'-phase structure of Nd_2CuO_4.[1] From the magnetic point of view the Cu lattice presents three-dimensional antiferromagnetic (AF) order for all cuprates below $T_N\approx$ 250–280 K.[2] For Gd_2CuO_4 and heavier rare-earth cuprates, the square array of oxygen ions surrounding the Cu sites is rotated around the c axis leading to a reduced orthorhombic symmetry.[3] The AF order is not perfect in this case and weak ferromagnetism (WF) appears for Gd through Yb compounds due to canting of the copper moments in the CuO_2 planes.[4–6] The origin of this canting has been attributed to an antisymmetric exchange interaction of the Dzyaloshinskii-Moriya (DM) type[7] allowed in this case by the orthorhombic distortion.

Early magnetization measurements in Gd_2CuO_4 single crystals[4,5] have shown a very strong out-of-plane anisotropy which favors the orientation of the WF component of the magnetization within the CuO_2 planes. In Ref. 5 it was suggested that the in-plane anisotropy was relative small (<15%). It was pointed out[8] that this small anisotropy is related with a special type of ordered oxygen displacement which allows an antisymmetric exchange interaction of the DM type.

In this paper we present a detailed study of the dc magnetization as a function of the applied field, which does show an important in-plane anisotropy for $H<H_c^*\approx 300$ G. This anisotropic behavior is described in Sec. III within a five sublattice magnetization model, four associated with the ordered Cu lattice and the other describing the Gd paramagnetic lattice.

II. EXPERIMENTAL RESULTS

We have made our measurements on a Gd_2CuO_4 single crystal, 4.7 mg of weight, grown by the flux technique.[4] The crystal has a platelike shape with the crystallographic c axis perpendicular to the plate. Magnetization measurements were made either with a Quantum Design superconducting quantum interference device magnetometer (in the 20–300 K range) or with a Digital Measurements vibrating sample magnetometer at 77 K.

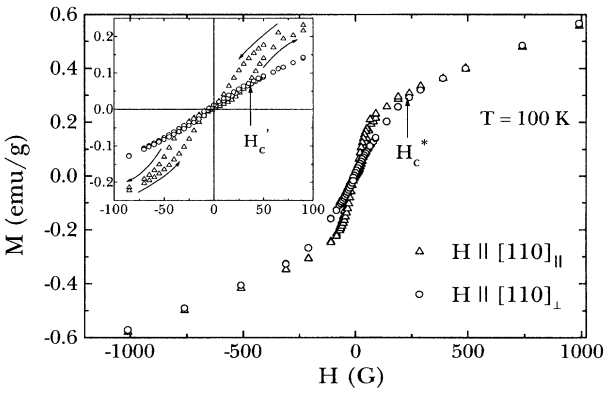

FIG. 1. Magnetization vs field cycles for $T=100$ K. Triangles and circles correspond to H applied parallel to $[110]_\parallel$ and $[110]_\perp$, respectively. H_c^* is the field necessary to align all moments parallel to the applied field. The inset shows a detail of the low field part of the curve. H_c' is the field where the metamagneticlike transition occurs. Magnetic hysteresis effects are observed in the ±75 G range.

In Fig. 1 we present magnetization data measured with H parallel and perpendicular to a [110] crystallographic direction at $T = 100$ K. Three different behaviors can be distinguished. For low fields ($0<H<H_c'\approx 35$ G) the magnetization is slightly anisotropic, being larger in the hard direction $[110]_\perp$ (see inset Fig. 1). At the critical field H_c', a sharp increase in the slope is observed for H applied parallel to the easy axis of magnetization $[110]_\parallel$. This critical field could be associated with a metamagneticlike transition in which spins of different planes, pointing opposite for $H=0$, line up. A similar behavior has been observed in polycrystalline samples of Y_2CuO_4, Ho_2CuO_4, and Tb_2CuO_4, but the critical fields are considerably larger: $H_c'=$ 1500, 1300, and 300 G for Y, Ho, and Tb compounds, respectively, at $T=100$ K.[9–11] For intermediate fields, $H_c'<H<H_c^*\approx 300$ G, M becomes very anisotropic. $M_\parallel$ presents a sharp increase near H_c' while $M_\perp$ remains almost linearly dependent on H. When H is larger than H_c^* an isotropic behavior is again observed as the applied field is large enough to saturate the WF magnetization in both directions.

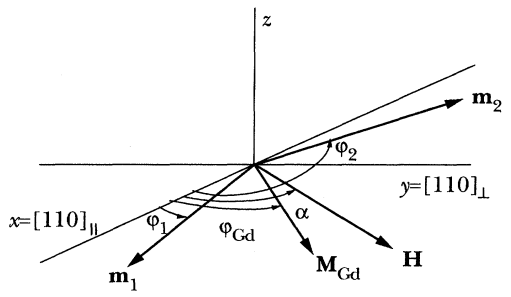

FIG. 2. Relative orientation of the uniform and Gd magnetic vectors and the external field. The axes of easy and hard magnetization are labeled $[110]_\parallel$ and $[110]_\perp$. The Cu sublattice magnetization vectors ($M_1,\ldots,M_4$), not drawn, are oriented almost parallel to the y direction in equillibrium.

III. DISCUSSION

A. Magnetic free energy

The magnetization of Gd_2CuO_4, when H is applied within the ab plane, is well described by[4]

$$\mathbf{M}=\mathbf{m}_{wf}+\chi_{Gd}(\mathbf{H}+\mathbf{H}_{i,Gd}), \tag{1}$$

where $\mathbf{m}_{wf}$ is the canted copper moment, $\chi_{Gd}=2C_{Gd}/(T+\theta)$ is the molar magnetic susceptibility of Gd ions, and $\mathbf{H}_{i,Gd}$ is the effective magnetic field acting on the Gd moments due to the coupling with the ordered Cu sublattice. It has been shown[12] that $\mathbf{H}_{i,Gd}$ is an almost linear function of $\mathbf{m}_{wf}$ through the relation $\mathbf{H}_{i,Gd}=\lambda'\mathbf{m}_{wf}$. Equation (1) is valid only for $H\geq 300$ G because $\mathbf{M}$ is not a linear function of $\mathbf{H}$ at low fields.

A phenomenological free energy, including symmetric and antisymmetric exchange interactions and second and fourth order anisotropy terms, was used to describe the magnetization and resonance modes of very diluted Gd cuprates.[13,14] In that case it was enough to consider only the interaction between two AF copper sublattices. It was shown there that, due to the high value of the symmetric exchange field and the added effect of a strong out-of-plane anisotropy and the antisymmetric exchange field, an effective free energy may be written for the uniform magnetization, $\mathbf{m}_{wf}$, reducing the problem to that of one WF lattice.

For concentrated Gd samples the coupling between the Gd and the Cu lattices needs to be taken into account. In order to do so, a three sublattice model including an isotropic ferromagnetic interaction between the Cu magnetization and the paramagnetic Gd sublattice was succesfully used.[15,16] However, a thorough description of the low field part ($H<300$ G) of the $\mathbf{M}$ vs $\mathbf{H}$ curves is still missing, specially when $\mathbf{H}$ is applied parallel to the easy axis of magnetization.

We show here that a better description may be obtained by considering explicitly the coupling between the Cu moments in CuO_2 planes separated by a distance $c/2$. The free energy should now include at least four Cu and one Gd sublattices

$$F=F_{Cu}+F_{Gd}+F_{Cu\text{-}Gd}, \tag{2}$$

with

$$4F_{Cu}=K_z\left[\sum_{i=1}^{4}(\mathbf{M}_i\cdot\hat{z})^2\right]-K_x\left[\sum_{i=1}^{4}(\mathbf{M}_i\cdot\hat{x})^2\right]+K_{x4}\left[\sum_{i=1}^{4}(\mathbf{M}_i\cdot\hat{x})^4\right]+\lambda[\mathbf{M}_1\cdot\mathbf{M}_2+\mathbf{M}_3\cdot\mathbf{M}_4]+\mathbf{D}\cdot[\mathbf{M}_1\times\mathbf{M}_2-\mathbf{M}_3\times\mathbf{M}_4]$$
$$+\lambda_\perp[\mathbf{M}_1\cdot\mathbf{M}_3+\mathbf{M}_2\cdot\mathbf{M}_4]-\sum_{i=1}^{4}(\mathbf{M}_i\cdot\mathbf{H}), \tag{3}$$

$$F_{Gd}=\left(\frac{1}{2\chi_{Gd}}\right)M_{Gd}^2-\mathbf{M}_{Gd}\cdot\mathbf{H}, \tag{4}$$

$$F_{Cu\text{-}Gd}=-\frac{\lambda'}{4}(\mathbf{M}_1+\mathbf{M}_2+\mathbf{M}_3+\mathbf{M}_4)\cdot\mathbf{M}_{Gd}. \tag{5}$$

F_{Cu} and F_{Gd} are the individual free energies of the ordered copper and the Gd paramagnetic sublattices, respectively. $F_{Cu\text{-}Gd}$ represents the exchange coupling between the two subsystems as in Ref. 16. The constants K_z, K_x, and K_{x4} (all >0) are second and fourth order magnetic anisotropy terms; λ, $\lambda_\perp$, and λ' (all >0) are the intraplanar, interplanar, and Cu-Gd

isotropic exchange interaction constants; **D** is the antisymmetric exchange vector corresponding to the DM interaction; and χ_{Gd} is the molar magnetic susceptibility of Gd ions, as in Eq. (1). Terms of the form $\mathbf{M}_i\cdot\mathbf{H}$ correspond to the Zeeman interaction with an external magnetic field.

Equation (2) may be rewritten in terms of the uniform and staggered magnetizations,[14]

$$\mathbf{m}_1=\frac{\mathbf{M}_1+\mathbf{M}_2}{4},\quad \mathbf{m}_2=\frac{\mathbf{M}_3+\mathbf{M}_4}{4},\quad \mathbf{l}_1=\frac{\mathbf{M}_1-\mathbf{M}_2}{4},\quad \mathbf{l}_2=\frac{\mathbf{M}_3-\mathbf{M}_4}{4}, \tag{6}$$

the equation for the free energy then becomes

$$\begin{aligned}F=&K_z\{[(\mathbf{m}_1+\mathbf{l}_1)\cdot\hat{z}]^2+[(\mathbf{m}_1-\mathbf{l}_1)\cdot\hat{z}]^2+[(\mathbf{m}_2+\mathbf{l}_2)\cdot\hat{z}]^2+[(\mathbf{m}_2-\mathbf{l}_2)\cdot\hat{z}]^2\}-K_x\{[(\mathbf{m}_1+\mathbf{l}_1)\cdot\hat{x}]^2+[(\mathbf{m}_1-\mathbf{l}_1)\cdot\hat{x}]^2\\&+[(\mathbf{m}_2+\mathbf{l}_2)\cdot\hat{x}]^2+[(\mathbf{m}_2-\mathbf{l}_2)\cdot\hat{x}]^2\}+4K_{x4}\{[(\mathbf{m}_1+\mathbf{l}_1)\cdot\hat{x}]^4+[(\mathbf{m}_1-\mathbf{l}_1)\cdot\hat{x}]^4+[(\mathbf{m}_2+\mathbf{l}_2)\cdot\hat{x}]^4+[(\mathbf{m}_2-\mathbf{l}_2)\cdot\hat{x}]^4\}\\&+\lambda[(\mathbf{m}_1+\mathbf{l}_1)\cdot(\mathbf{m}_1-\mathbf{l}_1)+(\mathbf{m}_2+\mathbf{l}_2)\cdot(\mathbf{m}_2-\mathbf{l}_2)]+\mathbf{D}\cdot[(\mathbf{m}_1+\mathbf{l}_1)\times(\mathbf{m}_1-\mathbf{l}_1)-(\mathbf{m}_2+\mathbf{l}_2)\times(\mathbf{m}_2-\mathbf{l}_2)]\\&+\lambda_\perp[(\mathbf{m}_1+\mathbf{l}_1)\cdot(\mathbf{m}_2+\mathbf{l}_2)+(\mathbf{m}_1-\mathbf{l}_1)\cdot(\mathbf{m}_2-\mathbf{l}_2)]-(\mathbf{m}_1+\mathbf{m}_2)\cdot\mathbf{H}+\left(\frac{1}{2\chi_{\mathrm{Gd}}}\right)M_{\mathrm{Gd}}^2-\mathbf{M}_{\mathrm{Gd}}\cdot\mathbf{H}-\lambda'(\mathbf{m}_1+\mathbf{m}_2)\cdot\mathbf{M}_{\mathrm{Gd}}.\end{aligned} \tag{7}$$

As for Gd_2CuO_4, $\lambda\gg D\gg(K_x,\lambda',H/M_0)$, $\mathbf{m}_{1,2}$ and $\mathbf{l}_{1,2}$ remain both in the *ab* plane (see Ref. 14), and their magnitudes are given by

$$|l_1|=|l_2|=|l|\approx\frac{M_0}{2},\quad |m_1|=|m_2|=|m|=\left|\frac{m_{\mathrm{wf}}}{2}\right|\approx\frac{D}{2\lambda}l, \tag{8}$$

and, as $|\mathbf{M}_i|=|\mathbf{M}_j|=|\mathbf{M}_0|$ implies $\mathbf{m}_i\perp\mathbf{l}_i$, an effective free energy can be written[14]

$$\begin{aligned}\frac{F_{\mathrm{eff}}}{m}=&-\frac{H_x}{2}(\cos^2\varphi_1+\cos^2\varphi_2)+H_{x4}(\cos^4\varphi_1+\cos^4\varphi_2)+H_e\cos(\varphi_1-\varphi_2)-H[\cos(\varphi_1-\alpha)+\cos(\varphi_2-\alpha)]\\&-\lambda' M_{\mathrm{Gd}}[\cos(\varphi_1-\varphi_{\mathrm{Gd}})+\cos(\varphi_2-\varphi_{\mathrm{Gd}})]+\frac{1}{m}\left(\frac{1}{2\chi_{\mathrm{Gd}}}M_{\mathrm{Gd}}^2-M_{\mathrm{Gd}}H\cos(\varphi_{\mathrm{Gd}}-\alpha)\right),\end{aligned} \tag{9}$$

where the effective fields are defined through $H_x=2K_xM_0(2\lambda/D)$, $H_{x4}=K_{x4}M_0^3(2\lambda/D)$, and $H_e=\lambda_\perp M_0(2\lambda/D)$. The angles φ_1, φ_2, φ_{Gd}, and α, measured with respect to the x axis, the easy axis for the uniform magnetization, are defined in Fig. 2. Terms not dependent on the angular variables have been omitted. The equilibrium orientation and magnitude for the magnetization of different sublattices is found by minimizing the total free energy with respect to the angular variables. The following set of coupled equations is obtained:

$$\begin{aligned}&\tan\varphi_{\mathrm{Gd}}=\frac{H\sin\alpha+\lambda' m(\sin\varphi_1+\sin\varphi_2)}{H\cos\alpha+\lambda' m(\cos\varphi_1+\cos\varphi_2)},\\&|M_{\mathrm{Gd}}|^2=\chi_{\mathrm{Gd}}^2\{H^2+2(\lambda' m)^2[1+\cos(\varphi_1-\varphi_2)]+2H\lambda' m[\cos(\varphi_1-\alpha)+\cos(\varphi_2-\alpha)]\}^2,\\&H_x\sin\varphi_1\cos\varphi_1-4H_{x4}\cos^3\varphi_1\sin\varphi_1-H_e\sin(\varphi_1-\varphi_2)+H\sin(\varphi_1-\alpha)+\lambda' M_{\mathrm{Gd}}\sin(\varphi_1-\varphi_{\mathrm{Gd}})=0,\\&H_x\sin\varphi_2\cos\varphi_2-4H_{x4}\cos^3\varphi_2\sin\varphi_2+H_e\sin(\varphi_1-\varphi_2)+H\sin(\varphi_2-\alpha)+\lambda' M_{\mathrm{Gd}}\sin(\varphi_2-\varphi_{\mathrm{Gd}})=0.\end{aligned} \tag{10}$$

For H applied parallel to $[110]_\parallel$ a metamagneticlike transition is expected at a critical field

$$H_c'=\frac{H_e-\xi\lambda' m}{1+\xi}=\frac{H_e-\xi H_{i,\mathrm{Gd}}/2}{1+\xi}, \tag{11}$$

with $H_{i,\mathrm{Gd}}=\lambda' m_{\mathrm{wf}}=2\lambda' m$, $\xi=\chi_{\mathrm{Gd}}\lambda'$. This critical field indicates the flipping of the copper moments from an antiparallel to a parallel alignment with respect to H. For the measured parameters a spin-flop-like transition is not expected to occur.

When H is applied parallel to $[110]_\perp$ a spin reorientation transition occurs at a critical field H_c^*.[14] The following expression could be deduced from Eq. (10):

$$H_c^*=\frac{2H_e-\xi H_{i,\mathrm{Gd}}/2+H_x}{1+\xi}=2H_c'+\frac{H_x}{1+\xi}. \tag{12}$$

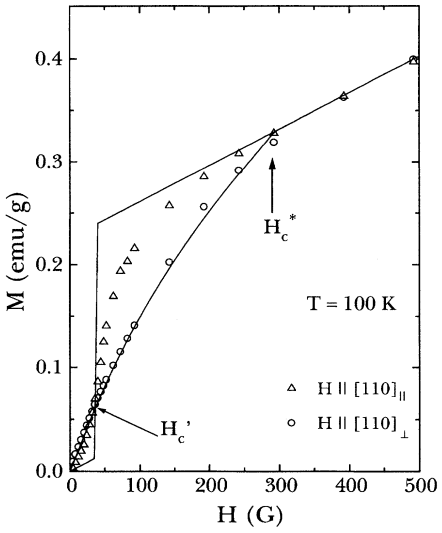

FIG. 3. First magnetization curve as a function of the applied field. Triangles and circles are data measured with H applied parallel to $[110]_{\|}$ and $[110]_{\perp}$. The solid line corresponds to a fit using Eq. (10).

From Eqs. (11) and (12) the interplanar exchange constant and the in-plane anisotropy field could be derived,

$$\lambda_{\perp}=\frac{H_e}{m_{\rm wf}}\left(\frac{D}{2\lambda}\right)^2=\frac{1}{m_{\rm wf}}\left(H_c'+\xi\left(H_c'+\frac{H_{i,\rm Gd}}{2}\right)\right)\left(\frac{D}{2\lambda}\right)^2, \tag{13}$$

$$H_x=(1+\xi)(H_c^*-2H_c'). \tag{14}$$

B. Data analysis

Using Eq. (10) we have fitted the first magnetization curves in both directions and the results are shown in Fig. 3. From the values of $D/2\lambda=9\times10^{-3}$, $H_{i,\rm Gd}=520$ G, $m_{\rm wf}=3.3\times10^{-3}$ G/(μ_β/Cu atom), and $\xi=4.4$ (at $T=100$ K) found in the literature,[4,5,12–14] and with $H_c'\approx35$ G and $H_c^*\approx300$ G obtained from the experimental data, we derive $H_x\approx1200$ G, $H_{x4}\approx175$ G, and $\lambda_{\perp}\approx$ 34.4 G/(μ_β/Cu atom), which gives $J_{\perp}\approx2.3$ mK. Note that the values determined for H_x and $J_{\perp}$ are considerably increased when the Cu-Gd interaction is taken into account [see Eqs. (13) and (14)]. If no coupling is included we would have obtained $H_x\approx225$ G and $J_{\perp}\approx0.06$ mK. The value of $J_{\perp}$ obtained is an order of magnitude smaller than those found in nonmagnetic Y_2CuO_4 (Ref. 9) ($J_{\perp}\approx16$ mK) and La_2CuO_4 (Ref. 17) ($J_{\perp}\approx23$ mK).

It should be mentioned that the magnetization in the $[110]_{\|}$ direction is not exactly steplike as the model predicts. A displacement of the out-of-plane oxygen, O(2), has been observed[3] by neutron difraction. This oxygen induces the coupling between neighboring planes, and slightly different displacements can originate a distribution of H_c' around a mean value causing a smoother curve. In the $[110]_{\|}$ direction hysteresis effects are observed in the ±75 G range (see inset Fig. 1), although with zero remanent magnetization and coercive field. Similar hysteresis effects in the hard axis direction are negligible. This hysteretic behavior is indicative of the presence of WF domains and could also be responsible, due to the effect of domain wall motion and reversal, for the smoother step at the critical field.

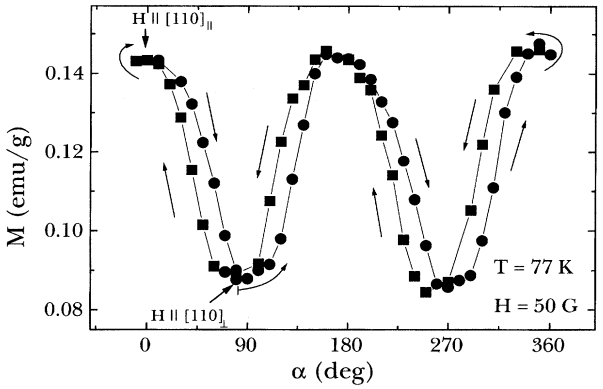

FIG. 4. In-plane angular variation of the magnetization measured at $T=77$ K with 50 G of applied field. See that $M_{\|}$ is almost twice as large as $M_{\perp}$. Arrows and different symbols indicate the measurement sequence. Note that strong angular hysteresis effects are present when H is not applied parallel to a $\langle110\rangle$ axis.

The in-plane anisotropy can be appreciated in Fig. 4. The angular variation, measured at 77 K with an applied field of 50 G, shows clearly that $M_{\|}$ is almost twice as large as $M_{\perp}$. Angular hysteresis effects are present when H is not applied parallel to a [110] direction. This is also indicative of the presence of WF domains.

Bordet *et al.*[18] have found three different types of superstructures associated with the long-range order of the CuO_2 plane distortions. In Ref. 8, Stepanov *et al.* analyzed the possible displacements of the oxygen atoms within the CuO_2 planes that could lead to WF. They show that two types of oxygen displacements perpendicular to the CuO chains exist.

Type 1 originates a completely isotropic magnetization within the *ab* plane for all applied fields and is related to the DM exchange interaction. Type 2, on the other hand, leads to an anisotropic magnetization in the *ab* plane with 180° symmetry. Based on the isotropic behavior of M at high fields, they concluded that type 1 was probably the distortion present. However, the fact that the magnetization measured at low fields is anisotropic led us to consider type 2 distortions as the most probable, adding to the free energy of Eq. (2) the following term: $D_2(M_{1x}M_{1y}-M_{2x}M_{2y}+M_{3x}M_{3y}-M_{4x}M_{4y})$. This contribution adds to Eq. (9) a term of the form $H_{D_2}(\cos^2\varphi_1+\cos^2\varphi_2)$. Such an expression accounts for the fact that type 2 distortions cause an easy axis of magnetization and may justify the phenomenologically introduced crystallographic anisotropy.

The ratio $M_{\|}/M_{\perp}$ is plotted in Fig. 5(a) as a function of T for $H=100$ G. This quantity serves as a parametrization of the anisotropy. A maximum is observed near $T=100$ K. In Fig. 5(b) we show the variation of $M_{\|}/M_{\perp}$ vs H at $T=100$ K. The maximum corresponds to $H\approx100$ G. We have defined the critical field H_c' as the data point where $M_{\|}/M_{\perp}$ crosses 1, and H_c^* when $M_{\|}/M_{\perp}$ reaches ≈1.02. In Fig. 6 we present the temperature dependence of H_c^*. This critical field increases with T, in agreement with Eq. (12), assuming

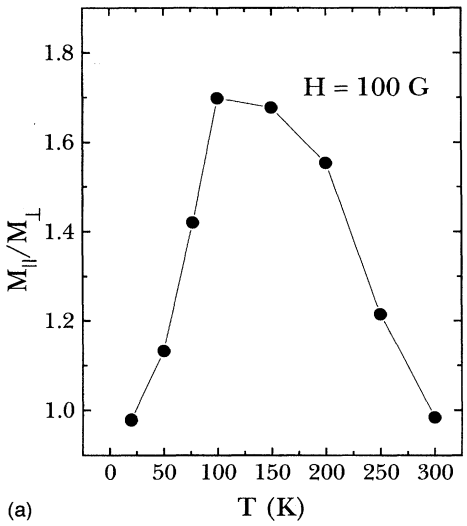

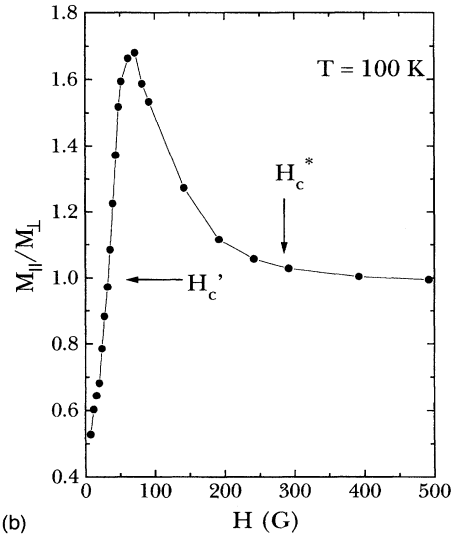

FIG. 5. Temperature (a) and field (b) variation of the factor $M_{\|}/M_{\perp}$ for $H=100$ G and $T=100$ K, respectively. This factor is representative of the amount of crystalline anisotropy.

that all parameters are almost temperature independent at low T, except $\chi_{\mathrm{Gd}}(T)$. The decrease in H_c^*, for $T>150$ K, indicates that the temperature dependence of the parameters used is important above this temperature and should be taken into account. The other critical field, H_c', does not present any significant temperature variation below T_N and remains nearly constant, $H_c' \approx 35$ G.

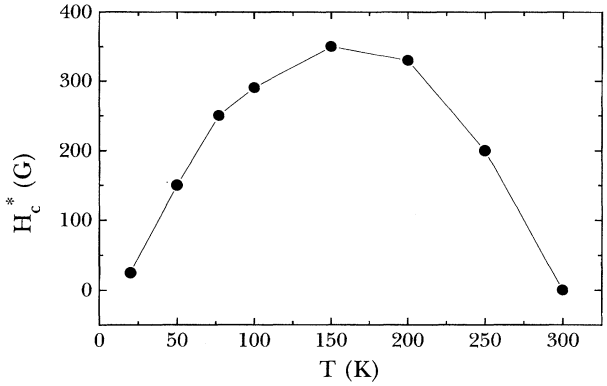

FIG. 6. Dependence of H_c^* with temperature. The increasing behavior for low T is consistent with Eq. (12) assuming that all parameters are almost temperature independent except for $\chi_{\mathrm{Gd}}(T)$. For higher temperatures a decrease in H_c^* is expected because it should equal zero at T_N.

IV. CONCLUSIONS

Detailed magnetization measurements have been made in order to study the existence of in-plane magnetic anisotropy in Gd_2CuO_4. We have shown that a metamagneticlike transition is present at fields much lower than that found in heavier rare-earth cuprates ($H_c' \approx 35$ G). In Ref. 11 it was suggested that the decrease in H_c' was related to the increase in the c-axis lattice parameter. Added to the variation of c, the effect of the displacements of the O(2) out-of-plane ions, which are smaller when c increases, may affect the magnetic behavior of the system. Apparentely the Gd compound has a c distance near the limit that prevents the occurrence of the metamagnetic transition. This may be related with the sample dependence of the magnetic properties observed esspecially for low magnetic fields. The interplanar exchange constant, $J_{\perp}$, is significantly smaller, only 10%, than those derived for non-magnetic cuprates. A relatively large anisotropy has been measured in the *ab* plane. This would imply a distortion of the oxygen squares different from that leading to a DM interaction. The observed behavior is consistently described within a five sublattice magnetic free energy model which takes into account the Cu-Gd coupling and the interaction between the Cu planes.

ACKNOWLEDGMENTS

One of us, A.B., acknowledges support from CONICET (Argentina). We thank Cindy Maley for her kindly helping us with the VSM measurements at the CMRR center.

[1] Hk. Müller-Buschbaum and W. Wollschläger, Z. Anorg. Allg. Chem. **414**, 76 (1975).

[2] R. Saez Puche, M. Norton, and W. S. Glausinger, Mater. Res. Bull. **17**, 1523 (1982); R. Saez Puche, M. Norton, T. R. White, and W. S. Glausinger, J. Solid State Chem. **50**, 281 (1983).

[3] M. Braden, W. Paulus, A. Cousson, P. Vigoureux, G. Heger, A. Goukassov, P Bourges, and D. Petitgrand, Europhys. Lett. **25**, 625 (1994).

[4] J. D. Thompson, S.-W. Cheong, S. E. Brown, Z. Fisk, S. B. Oseroff, M. Tovar, D. C. Vier, and S. Schultz, Phys. Rev. B **39**, 6660 (1989).

[5] S. B. Oseroff, D. Rao, F. Wright, M. Tovar, D. C. Vier, S. Schultz,

J. D. Thompson, Z. Fisk, and S.-W. Cheong, Phys. Rev. B **41**, 1934 (1990).

[6] M. Tovar, X. Obradors, F. Perez, S.B. Oseroff, R. J. Duro, J. Rivas, D. Chateigner, P. Bordet, and J. Chenavas, Phys. Rev. B **45**, 4729 (1992).

[7] I. E. Dzyaloshinskii, J. Chem. Phys. Solids **4**, 241 (1958); T. Moriya, in *Magnetism*, edited by G. T. Rado and H. Suhl (Academic Press, New York, 1966), Vol. 1, p. 85.

[8] A. A. Stepanov, P. Wyder, T. Chattopadhyay, P. J. Brown, G. Fillion, I. M. Vitebsky, A. Deville, B. Gaillard, S. N. Barilo, and D. I. Zhigunov, Phys. Rev. B **48**, 12979 (1993); I. M. Vitebskii and A. A. Stepanov, J. Low Temp. Phys. **19**, 160 (1993).

[9] A. Rouco, X. Obradors, M. Tovar, P. Bordet, D. Chateigner, and J. Chenavas, Europhys. Lett. **20**, 651 (1992).

[10] A. Rouco, X. Obradors, M. Tovar, F. Pérez, D. Chateigner, and P. Bordet, Phys. Rev. B. **50**, 9924 (1994).

[11] A. Rouco, Ph.D. thesis, Universitat de Barcelona, España, 1994.

[12] L. B. Steren, M. Tovar, and S. B. Oseroff, Phys. Rev. B **46**, 2874 (1992).

[13] R. D. Zysler, A. Butera, A. Fainstein, M. Tovar, and Z. Fisk, J. Appl. Phys. **73**, 5680 (1993).

[14] A. Fainstein, A. Butera, R. D. Zysler, M. Tovar, C. Rettori, D. Rao, S. B. Oseroff, Z. Fisk, S.-W. Cheong, D. C. Vier, and S. Schultz, Phys. Rev. B **48**, 16775 (1993).

[15] A. Fainstein, M. Tovar, and Z. Fisk, J. Phys. Condens. Matter **4**, 1581 (1992).

[16] A. Fainstein, A. Butera, and M. Tovar, Phys. Rev. B **50**, 16708 (1994).

[17] S-W. Cheong, J. D. Thompson, and Z. Fisk, Phys. Rev. B **39**, 4395 (1989).

[18] P. Bordet, J. J. Capponi, C. Chaillout, D. Chateigner, J. Chenevas, Th. Fournier, J. L. Hodeau, M. Marezio, M. Perroux, G. Thomas, and A. Varela, Physica C **193**, 178 (1992).